International Journal on Interactive Design and Manufacturing (IJIDeM)
https://doi.org/10.1007/s12008-024-02087-4

ORIGINAL ARTICLE

Design for assembly principles applied to deformable parts, a natural frequency based methodology for interfaces design

Mattia Maltauro[1] · **Elisa Vargiu**[2] · **Roberto Meneghello**[2] · **Gianmaria Concheri**[1]

Received: 4 March 2024 / Accepted: 20 August 2024

Abstract

In this paper, a possible application of the DfA (Design for Assembly) principles to deformable parts is proposed. The efficiency of an assembly is expressed with the DfA index, which is influenced by the number of parts compared to the "minimum number of parts" and the assembly time. Deformable parts, if unsupported, can exhibit deformations outside functional limits; however, when assembled, they often need to behave like rigid parts. To achieve the necessary rigidity, a large number of constraints are added. Having a high number of anchor points between a part and the rest of the assembly induces a high assembly time and therefore a low DfA index. This paper aims to provide a methodological framework for designers to define optimal anchor point locations to achieve the desired rigidity with the minimum number of anchor points possible, thereby minimizing assembly time and maximizing the DfA Index. The procedure is based on modal analysis. Subsequent anchor points are added until the predefined rigidity measure, as the natural frequency, is reached. The procedure is validated through a simple case study and then applied to two cases derived from actual industrial applications. It is also shown how the procedure allows for an actual reduction of anchor points.

Keywords DfA · Design for assembly · Deformable parts · Modal analysis · Product architecture · Mechanical interface design · Constraints optimization

1 Introduction

Deformable parts are becoming increasingly common in everyday products. Thin-walled metal or plastic parts are found in nearly every engineered product, including appliance covers, car dashboards, bodywork, etc. Using thin-walled components allows for lighter products that are easier to handle and more environmentally friendly, as less material is used and better fuel consumption, therefore less CO_2 emissions can be achieved for vehicles [1, 2].

Among thin-walled structures, shell-like structures receive emphasis. Homogeneous shells and honeycomb sandwich plates are commonly encountered [3]. Considering homogeneous thin-walled structures, the thin-walled properties are relevant at the macroscopic scale. In contrast, honeycomb sandwich plates exhibit thin-walled properties at a lower scale, with the main plate defined by a composition of plates at a lower scale. Honeycomb cells are used to create thin-walled structural elements that combine rigidity with lightness and other customizable mechanical behaviours [4]. This study focuses on homogeneous thin-walled structures only.

A thin-walled homogeneous part, if unsupported, may lack rigidity and bend under its own weight, rendering it unable to support external loads without buckling. However, the final product, i.e., the assembly, typically needs to be rigid for ease of handling by the end-user. Nevertheless, parts included in the assembly may be produced as

✉ Mattia Maltauro
mattia.maltauro@unipd.it

Elisa Vargiu
elisa.vargiu@phd.unipd.it

Roberto Meneghello
roberto.meneghello@unipd.it

Gianmaria Concheri
gianmaria.concheri@unipd.it

[1] Department of Civil, Environmental and Architectural Engineering, Laboratory of Design Methods and Tools in Industrial Engineering, University of Padova, Via Venezia 1, Padova 35131, Italy

[2] Department of Management and Engineering, University of Padova, Stradella San Nicola 3, Vicenza 36100, Italy

Published online: 30 August 2024

deformable parts. This implies that the part is deformable in its free state but becomes stable and rigid once assembled [5].

When dealing with deformable parts, extensive literature about the optimization of clamping location and or sequence can be found. The aim is to limit and control geometrical variations of the final assembly. These methodology are based on Finite Element Method simulation (FEM). Most contributions deal with sheet metal parts and assemblies commonly found in the automotive and aerospace sectors. Sellem and Rivière propose a mechanical approach using influence coefficient matrices to compute tolerances for welded, bolted, riveted, or glued sheet metal parts [6]. Liu and Hu introduce an "offset finite element model" to predict assembly variability in spot-welded sheet metal parts [7]. Liu, Hu, and Woo discuss differences between "series" and "parallel" assemblies, finding lower variability in parallel assemblies [8]. The Influence Coefficient method, which links the assembly's spring-back to its free-state condition, was developed to determine the "as assembled" configuration [9]. This method was further refined to account for shape defects and contact modelling [10, 11]. A comprehensive summary of these methodologies is available in the literature [12].

Regarding the optimization of the assembly process for deformable parts, it must be considered that these parts endure deformation during the assembly. Typically, the final configuration of the part is ideally reflected in the fixturing system used in the assembly station which imposes an over-constrained deformation [9]. The assembly process for a deformable part is commonly made of four steps: the part is positioned in the fixture (isostatically), the part is iperstatically clamped, the parts are joined together, and finally the assembly is released from the fixture [13].

Different steps of the assembly process were previously covered such as the fixture design [14–16], the clamping procedure [17–19], and also welding distortion [20–23]. Parallelly, the optimization of these steps has been presented [24–27].

All these methodologies pertain to the manufacturing stage of the product. The parts' geometry, and their mutual interfaces, are already defined. The free variables are, on one side, the manufacturing tolerances; on the other, the assembly tooling and or sequence.

Methodology to deal with deformable parts during inspection was also explored. Radvar-Esfahlan and Tahan present the Generalized Numerical Inspection Fixture (GNIF) for fixtureless inspections of freeform surfaces on non-rigid thin-walled parts [28]. This method assumes isometric deformation, maintaining constant geodesic distances between internal points during deformation. Correspondent points between the CAD model and the freeform acquired model are defined using this assumption. Subsequent improvements to this framework include enhanced boundary conditions and automation [29, 30]. To address the loss of information in a fully clamped configuration, Lindau et al. proposed measuring with a three-point support setup, simulating the clamped state via FEM simulation and the influence coefficient method [31]. Morse and Grohol contributed an efficient methodology for fixtureless inspection of non-rigid parts by performing FEM simulation on nominal geometry independently of actual data [32].

In this paper, the focus is on the design phase. Specifically the nominal design phase. Geometrical variability is not considered at this stage. The aim is to design the nominal geometry of a deformable part considering the ease of assembly and the final rigidity of the product. Mechanical rigidity primarily depends on material properties (i.e., Young's modulus), part geometry (mass distribution), and external constraints. In this context, material and geometry are considered fixed, leaving constraint location (i.e., mechanical interfaces), as the sole degree of freedom for affecting part rigidity. Deformable parts require multiple anchor points to achieve stable, rigid configurations. The greater the number of anchor points, such as snap fits, rivets, or bolts, the more complex the assembly process becomes. If geometric tolerances are taken into account, it can be demonstrated that as the number of shaft hole elements that need to meet increases, the play between parts decreases, or the interference becomes greater [33]. Consequently, alignment becomes more precise, necessitating dedicated alignment tools and/or more time to achieve a usable alignment.

Traditional assembly methods, such as screws or bolts, result in increased assembly time proportional to the number of anchor points. Consequently, more anchor points inevitably lead to inefficient assembly procedures.

The Boothroyd-Dewhurst Design for Assembly (DfA) Method [34–37] offers a methodology for quantifying assembly efficiency. The DfA Index (%) primarily considers the number of parts in the assembly versus the minimum number required for the same functionality, as well as assembly time.

Increasing the number of anchor points in a deformable part reduces the DfA Index due to increased assembly time. Proper design of interfaces is thus necessary to increase the DfA index by minimizing assembly time, given fixed geometry and part count.

Since its introduction, the DfA method has been widespread in industry and over the years has been applied in many different fields of application [38], from the well-established automotive [39] and aerospace [40], up to the building construction sector [41, 42]. It has also been used to optimize assembly sequences [43]. To the best of the authors' knowledge no effort towards an application

dedicated to deformable parts considering the peculiarity of the interfaces required for such parts can be found.

Therefore, to fill this gap, this paper aims to maximize the DfA index for deformable components by designing anchor locations to minimize their number through a simulation-based approach. A methodology based on modal analysis during the design phase will be presented to minimize the number of anchor points needed to achieve a stable, sufficiently rigid configuration. The minimization of anchor points enables a simpler assembly process therefore minimising the assembly time leading to a higher DfA index. The same methodology will also be applied to redesign existing components to achieve the same rigidity with fewer anchor points.

The paper will present the methodology in Sect. 2, validate it in Sects. 3 and 4, and present increasingly complex case studies in Sect. 5, and conclude with discussions.

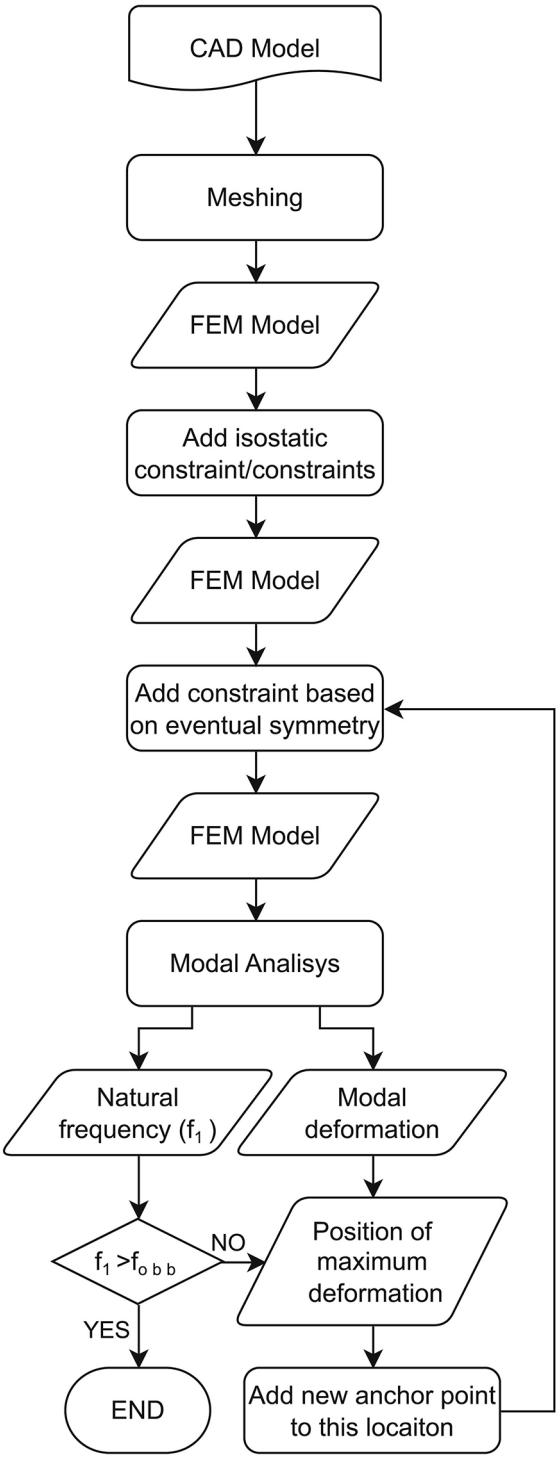

Fig. 1 Overall methodology

2 Tools and methods

The concept of rigidity is closely tied to the concept of natural frequency. A higher natural frequency indicates greater rigidity and lower deformations under the same external loading conditions [44–46]. Thus, it is possible to translate the problem of achieving a certain level of rigidity in the "as assembled condition" into the problem of attaining a predetermined natural frequency. The natural frequency depends on the part's intrinsic rigidity and the boundary conditions, i.e., the constraints. By adjusting the constraints, it is possible to alter the natural frequency of the "as assembled" part.

The overall methodology is illustrated in Fig. 1. In essence, starting from the CAD model of the part, a Finite Element Method (FEM) model is generated by appropriately meshing the geometry. The initial constraint, or set of constraints, is introduced to achieve an isostatic configuration. Subsequently, based on eventual symmetry conditions, additional constraints may be added to create a symmetrical model if needed in the design. Modal analysis is then conducted to determine both the first natural frequency and the associated modal deformation. If the first natural frequency exceeds the target natural frequency, the process concludes as a rigid configuration has been achieved. Conversely, if the modal deformation indicates otherwise, an additional constraint is applied at the location of the maximum modal deformation, and the process is iterated.

2.1 Preliminary steps

Before proceeding with the methodology, several preliminary steps are necessary: determining the target natural frequency in the constrained state, defining the symmetry of the part, establishing the domain in which anchor points can be placed to meet the adjacent parts, and identifying the initial point/points.

2.1.1 Target natural frequency determination

Firstly, the target natural frequency needs to be determined. Two main cases can be identified: the design case and the re-design case.

In the design case, which occurs when a new part for a new product needs to be designed, the aim is to avoid "over-engineering" the part by using more anchor points than necessary. In this scenario, the target natural frequency can be determined by analyzing previous designs of similar components that were sufficiently rigid. FEM simulations may also provide a valid alternative.

The re-design case involves a functional product that is already available, such as a product on the market or a working prototype. In this case, the geometry and anchor points of the part are already defined. If the rigidity of this part is satisfactory, it can serve as a baseline, and its natural frequency in the constrained state can be defined as the target for the re-design. Therefore, the objective is to determine whether the same rigidity, measured by the natural frequency, can be achieved using fewer anchors.

If the rigidity is unsatisfactory, a target natural frequency needs to be defined, similar to the design case. The methodology is then employed to maximize rigidity by adding one anchor point at a time.

It is not possible to provide general values for the target natural frequency. Each case study needs to be analyzed independently. The main usage of the presented tool is comparative, allowing to compare different design options, and or, comparing new designs with current solutions.

2.1.2 Symmetry determination

Part symmetry represents an important feature of parts optimized for the assembly process. A symmetric part requires fewer operations to be correctly aligned for assembly, thereby reducing assembly time [47]. While a part may possess various symmetry planes in its geometry when considered without anchor points, the random placement of anchor points can render the part asymmetric. Moreover, if the asymmetry results from the locations of anchor points, establishing the part's orientation becomes even more challenging, indeed the part can be considered as "slightly" asymmetrical or "almost-symmetrical" [47].

If the proposed procedure is applied without considering any symmetry constraints, the anchor point locations may be asymmetric even with a symmetric part. To address this issue, it is important to predetermine the symmetry conditions desired in the design. Symmetry conditions are not essential for running the proposed methodology, even if are important features of parts optimized according to the DfA principles. If symmetry conditions are requested, this requires adding symmetric anchor points corresponding to each anchor point added to the model. At each step, at least two anchor points are added, unless the anchor point coincides with the symmetry plane.

2.1.3 Admissible anchor point location

When designing anchor point locations, the position of adjacent parts needs to be considered. Therefore, anchor points cannot be placed randomly all over the part geometry. The determination of the area in which anchor points are allowed becomes crucial for the methodology.

2.1.4 Location of the initial point

To run the procedure, a starting point needs to be selected. The initial anchor/anchors configurations must be at least isostatic, meaning that they need to block all six degrees of freedom. If mandatory anchor points are needed, these must be used. If no mandatory anchor points are required, the initial condition can be chosen randomly by the designer. A more structured approach is represented by choosing the location through a free-state modal analysis. The first anchor point can be placed in the location of the maximum displacement associated with the first non-null natural frequency determined in the free state.

2.2 Implementation

The creation of the FEM model from the CAD geometry is a crucial step. Beam and shell elements should be preferred to obtain more representative results for the natural frequency of thin or slender parts, which are mostly subject to deformability before assembly.

Once the FEM model has been created (meshed with material properties), the first interesting test is to assess the maximum natural frequency that can be reached by considering the entire area where anchor points are allowed. This corresponds to a glueing process applied to the entire area. At this point, the first set of isostatic constraints needs to be added. If the type of anchor to be used is assimilated to an interlocking constraint, only one constraint can be added. Otherwise, a congruent number of constraints need to be added to lock all 6 degrees of freedom of the part. If mandatory anchor points are needed and defined in the preliminary phases, they need to be added even if they already represent a hyperstatic solution.

Contacts between parts are not considered allowing to perform linear modal analysis instead of non-linear analysis. It must be noted that this influences the final result. At the same time, as previously mentioned, the main usage of the presented methodology is comparative, therefore as

soon as the same simulation hypothesis are used the results can be compared and therefore design decisions can be made. Furthermore, being a design tool, the full interface geometry might not be available, therefore, it is not possible to appropriately account for contacts between parts.

Symmetries are then considered, and symmetric anchor points are added as needed.

The modal analysis is then performed. In this paper, PATRAN/NASTRAN is used to conduct FEM simulations (Normal modes, SOL 103). Both the first natural frequency and the corresponding translational deformation (Eigenvector) are recorded.

The natural frequency is compared to the target natural frequency. If the natural frequency is higher than the target, the component is considered rigid enough, and the anchor points defined so far are deemed optimal, concluding the design. If the natural frequency is lower than the target, the rigidity needs to be increased by adding additional anchor points. The additional anchor point is added at the location of the maximum eigenvector translation to block the corresponding deformation mode. The addition of this new constraint prevents the part from deforming according to the modal deformation. Being any possible deformation of a body the linear combination of all its modal deformations, by preventing the part from deforming according to a model deformation associated with a specific natural frequency, the new natural frequency of the part will be higher, therefore the rigidity increases.

A new modal analysis is performed, and the procedure is iterated.

3 Validation

To validate the approach, a series of sensitivity analyses are conducted on a simple planar rectangular plate measuring $200 \times 400\, mm^2$, with a thickness of $1\, mm$. The part is made of plastic (PLA) with the following mechanical properties: Young's modulus $E = 3.1\, GPa$, density $\delta = 1240\, kg/m^3$, Poisson's ratio $\nu = 0.3$. The anchors are allowed only along the external perimeters, positioned $5\, mm$ from the border. A schematic representation of the case is depicted in Fig. 2.

Both the cases considering the two median planes of symmetry and the non-symmetric case are evaluated to look for differences in performance. Five different starting points are considered: corner (case 1), short side midpoint (case 2), long side midpoint (case 3), short side random point (case 4), and long side random point (case 5). Figure 2 shows the positions of the initial points that were used. Therefore, a total of ten cases have been analyzed.

The proposed methodology has been followed for each of the cases up to at least twelve constraints in total. The increase in natural frequency is recorded and compared. The FEM mesh is defined by shell elements (CQUAD4) with dimensions of $5 \times 5\, mm^2$.

To check whether the added constraint is optimal, a sensitivity analysis is performed by changing the position of an additional constraint around the position indicated by the methodology.

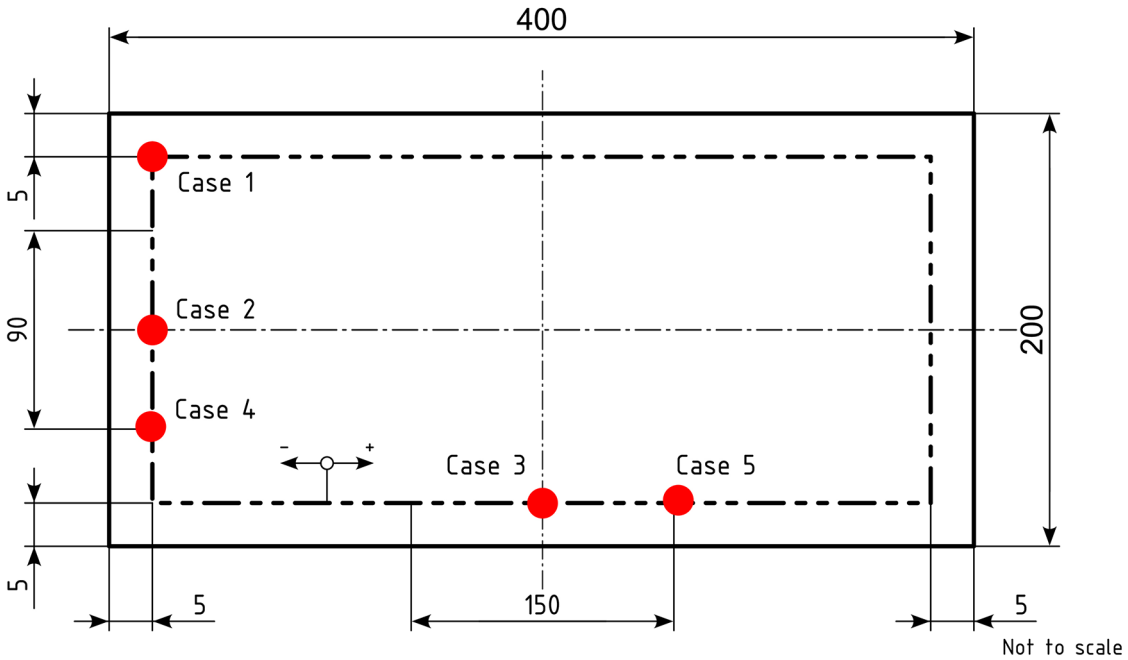

Fig. 2 Validation case geometry, admissible anchor point location, and starting point locations

Table 1 Natural frequencies obtained using symmetries

Case 1.1.		Case 1.2.		Case 1.3.		Case 1.4.		Case 1.5.	
Corner		Short side midpoint		Long side midpoint		Short side random		Long side random	
Constrains	f_n	Constrains	f_n	Constrains	f_n	Constrains	f_n	Constrains	f_n
2	-	2	6,60	2	3,36	2	-	2	-
4	7,41	4	18,78	4	18,78	4	8,33	4	10,80
6	23,48	6	-	6	-	6	26,79	6	30,22
8	32,05	8	27,38	8	27,38	8	-	8	-
10	-	10	-	10	-	10	35,11	10	31,56
12	35,89	12	35,89	12	35,89	12	-	12	37,35
14	-	14	-	14	-	14	35,86	14	-

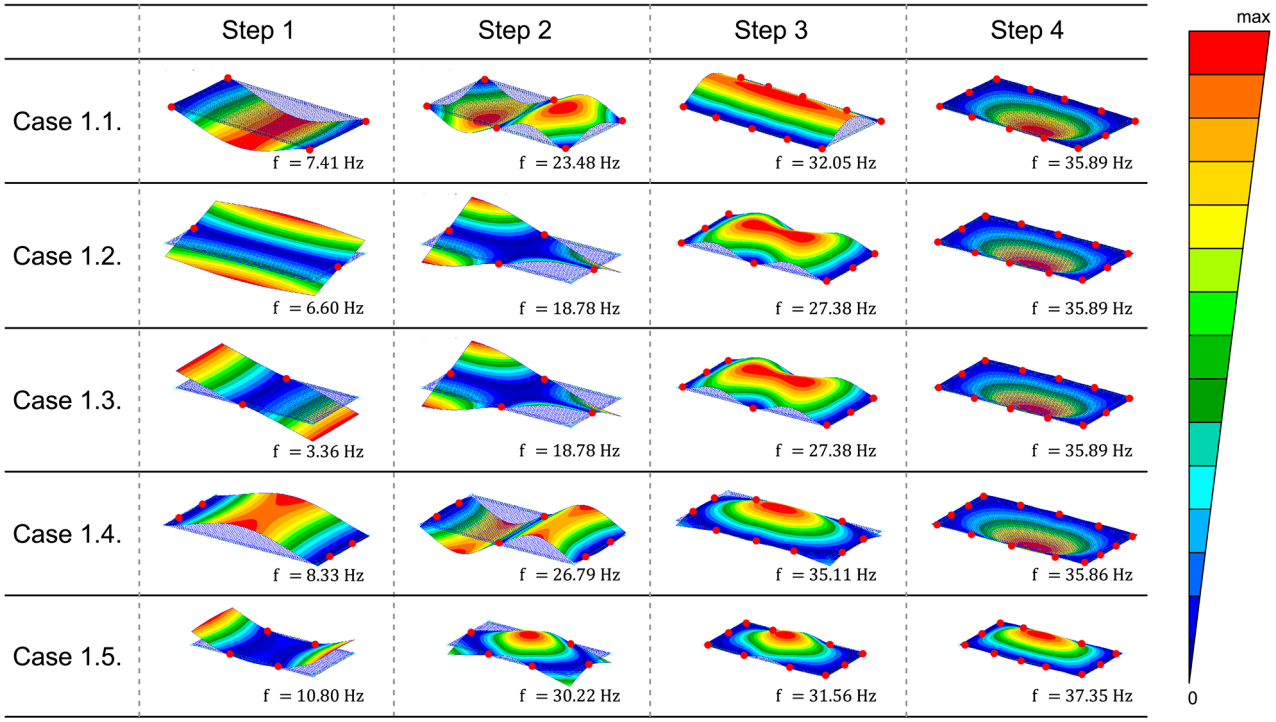

Fig. 3 Step-by-step convergence for the symmetric case

4 Results

The maximum natural frequency obtainable by blocking all nodes along the line where anchor points are allowed is $51.51\ Hz$.

The iteration results using symmetries are presented in Table 1. It can be noted that if the starting point coincides with a symmetry plane (Case 1.2. and 1.3.), or is placed in the corner (Case 1.1.), the procedure converges in four iterations to the same solution with twelve constraints. The step-by-step convergence can be seen in Fig. 3. Starting with a point in a random position (Case 1.4. and 1.5.), the iteration diverges from the previous cases. Referring to Case 1.4., the final result requires fourteen anchor points; the use of two additional anchor points does not imply a higher natural frequency, as seen for the random starting point on the short side. At the same time, the natural frequency reached with ten anchor points is not far from the one found applying the symmetry conditions.

The iterations obtained using the non-symmetries are presented in Table 2. In each case, twelve steps are required since one single anchor point is added per iteration. It can be noted that the natural frequency reached with twelve anchor points converges around $35\ Hz$, similar to the case with symmetry. In two cases, the procedure converges to the same solution: starting point in the corner and the long side midpoint. In these instances, the anchor points reach a quasi-symmetrical configuration; the symmetry is broken by just one anchor point location which is offset by a single node ($5\ mm$). Therefore, the solution might be considered

Table 2 Natural frequencies obtained without symmetries

Case 2.1.		Case 2.2.		Case 2.3.		Case 2.4.		Case 2.5.	
Corner		Short side midpoint		Long side midpoint		Short side random		Long side random	
Constrains	f_n	Constrains	f_n	Constrains	f_n	Constrains	f_n	Constrains	f_n
1	0,24	1	0,17	1	0,24	1	0,16	1	0,22
2	4,30	2	4,07	2	2,94	2	4,46	2	4,09
3	4,87	3	7,15	3	9,73	3	6,39	3	7,46
4	7,41	4	9,12	4	10,04	4	9,90	4	9,88
5	11,32	5	19,92	5	11,32	5	18,44	5	16,73
6	23,48	6	21,74	6	23,48	6	18,94	6	18,25
7	23,61	7	25,94	7	23,61	7	26,18	7	26,05
8	26,81	8	28,35	8	26,81	8	29,80	8	26,95
9	27,53	9	30,72	9	27,53	9	31,45	9	30,33
10	32,06	10	31,44	10	32,06	10	33,77	10	31,65
11	33,01	11	34,74	11	33,01	11	34,12	11	34,17
12	35,98	12	35,46	12	35,98	12	34,73	12	36,67

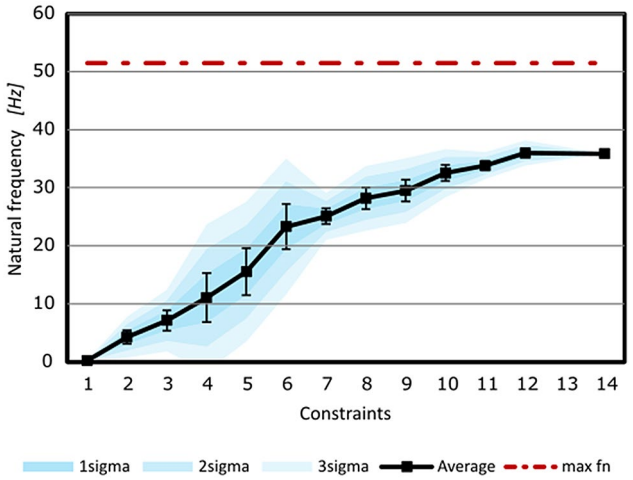

Fig. 4 Natural frequency dispersion considering all ten cases

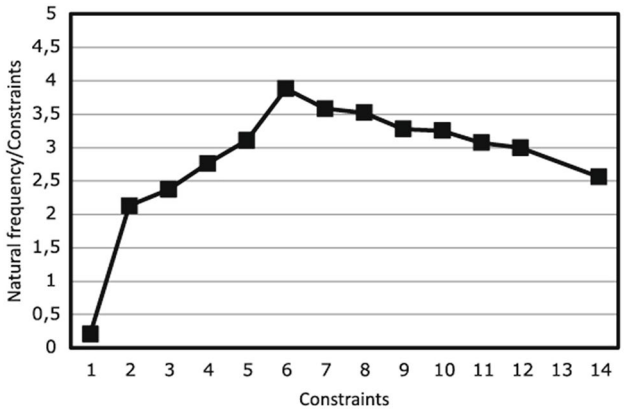

Fig. 5 Average natural frequency contribution of each anchor point as a function of the total number of constraints

symmetrical and modelled as such with minimal impact on the natural frequency.

Figure 4 shows the dispersion of the natural frequencies reached with different numbers of anchor points. It can be observed that the mean natural frequency as a function of the number of anchor points presents an asymptotic convergence to the maximum obtainable natural frequency. Consequently, the increase in natural frequency given by each additional constraint decreases as the total number of anchor points increases. This effect is also evident in Fig. 5, where the average contribution to the natural frequency for each anchor point is plotted as a function of the total number of constraints. It can be observed that six anchor points represent the most efficient configuration, in which each anchor point contributes the most to the rigidity of the part. Beyond that point, the average natural frequency provided by each constraint decreases in an almost linear manner.

From Fig. 4 it is also evident that the variability of the natural frequency is higher for a low number of anchor points, indicating that the result is less sensitive to initial conditions (symmetries and initial anchor point) with a higher number of anchor points. This effect is clearly illustrated in Fig. 6; from seven anchor points onwards, the dispersion (standard deviation) is approximately around 5% ($2\% < \sigma < 7\%$). For lower numbers of anchor points, the dispersion exceeds 15% of the mean value, reaching up to 38% for four anchor points.

In Fig. 7, the average natural frequencies obtained using symmetry and without symmetry are compared. It can be observed that the overall trend is similar, but for a low number of constraints, the use of symmetry appears to yield better results, which is particularly evident for four and six anchor points. For eight, ten, and twelve anchor points, no significant differences can be observed.

To test whether the additional anchor point placed in correspondence with the maximum translation deviation of the

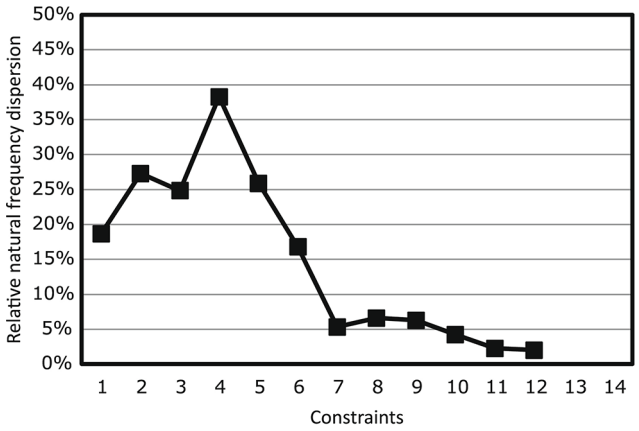

Fig. 6 Relative natural frequency dispersion, measured as standard deviation, as a function of the total number of constraints

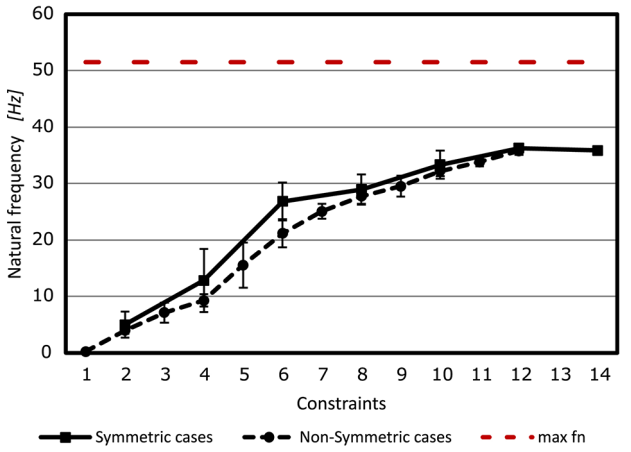

Fig. 7 Comparison between the average natural frequency obtained using symmetries and without using them

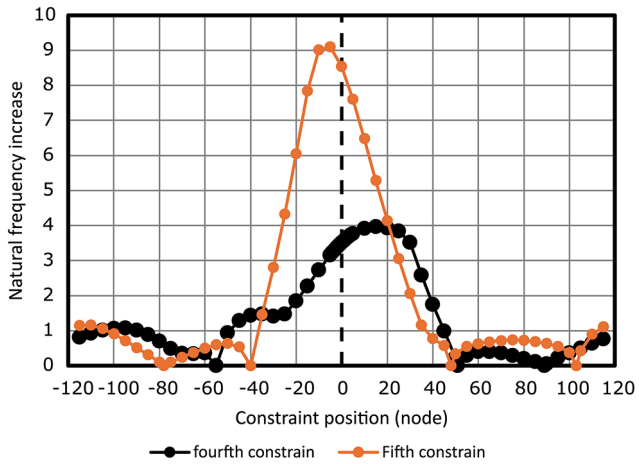

Fig. 8 Increase in natural frequency placing the additional anchor point around the point defined by the methodology, the x-axis represents the number of nodes from the node defined by the methodology in the anticlockwise direction along the admissible anchor point location (see Fig. 2 for reference)

eigenvector is the best possible solution, a test placing the anchor point around the one defined by the methodology is performed, and the results are shown in Fig. 8.

Testing the position of the fourth anchor point, defined without using symmetries and with a random starting point along the short edge (Case 2.4.), it can be seen that the additional anchor point is not in the optimal position, yet very close to the optimal position. The increase in natural frequency is around 10% less than the maximum obtainable. The same behaviour can be noted for the definition of the fifth anchor point; in this case, the difference with the optimal point position is even smaller.

5 Case studies

Two different case studies derived from actual industrial cases are investigated.

5.1 Washing machine back cover

The first case study is represented by a washing machine back cover. In Fig. 9 the actual geometry of the part, the simplified CAD Model, and the FEM model are depicted.

Being subject to vibration, the washing machine back cover needs to be rigid enough to prevent vibrations and noise during use. The current design incorporates a total of ten anchor points divided between clamps and screws, as highlighted in Fig. 9.a), for the sake of simplification, both anchors have been idealized with an interlocking constraint. The constraint location is idealized along a line with a $5\,mm$ offset from the external border, considered as the admissible anchor point location for the iterative process. The mesh is defined by shell elements (CQUAD4); a mesh seed of $5\,mm$ was set to have a node every $5\,mm$ along the admissible anchor point location. The thickness of the part is $2\,mm$, and the material has the following mechanical properties: $E = 2.3\,GPa$, $\delta = 1020\,kg/m^3$, $\nu = 0.38$.

Four different settings have been tested:

- Symmetric condition (plane x-z) and starting point over the symmetry plane (Sym. v01).
- Symmetric condition (plane x-z) and starting point defined by the free state modal analysis (Sym. v02).
- Non-symmetric condition (plane x-z) and starting point over the symmetry plane (Not Sym. v01).
- Non-symmetric condition (plane x-z) and starting point defined by the free state modal analysis (Not Sym. v02).

The results are summarized in Fig. 10. Here, the difference between the natural frequency and the maximum obtainable natural frequency is reported. The baseline result, obtained

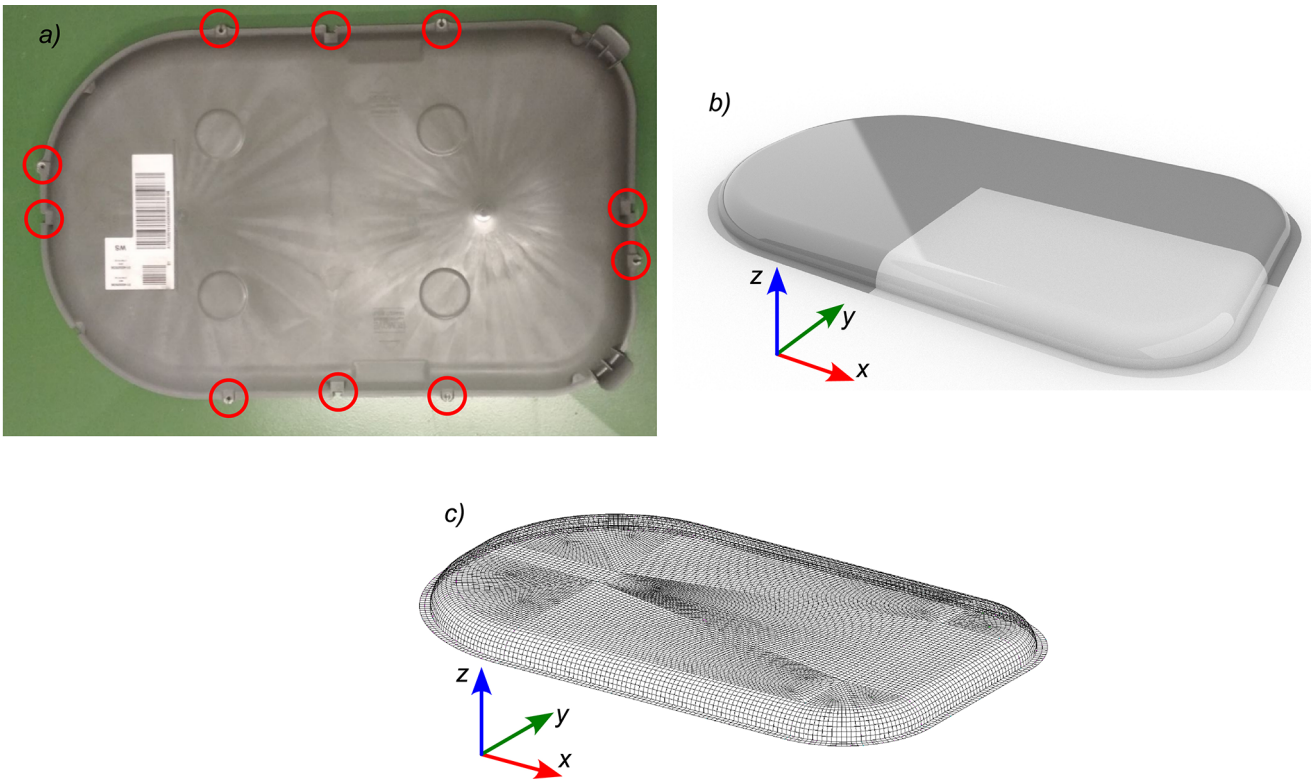

Fig. 9 First case study actual part (**a**), CAD model (**b**), and FEM model (**c**)

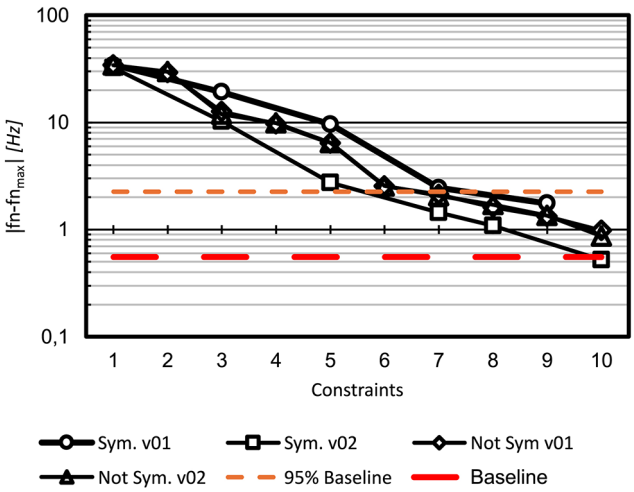

Fig. 10 First case study results

using the original constraint location and number (see Fig. 9) is $33.94\,Hz$ versus a maximum obtainable natural frequency of $34.50\,Hz$.

It can be noted that the non-symmetric cases are almost perfectly overlapped. A significant difference can be seen for the symmetric cases; the best starting point is the one obtained through a free-state modal analysis. It can also be seen that only in one case a natural frequency greater than the baseline is reached for the same number of constraints as the baseline: case Sym. v02 with a natural frequency of$33.97\,Hz$.

If 95% of the baseline natural frequency ($32.25\,Hz$) is considered as the goal (dashed orange line), it can be seen that three out of four conditions have a greater natural frequency using a total of seven constraints. Only the case Sym. v01 has a lower natural frequency ($32.05\,Hz$) with seven constraints.

5.2 Motorbike front fairing

The second case study looks at the front fairing of a motorbike. In Fig. 11 the actual geometry, the simplified CAD model, and the FEM model are presented.

In this case, the actual geometry was 3D scanned using an EinScan Pro HD. Using Fusion 360 from Autodesk, a NURBS polysurface was reverse-engineered. In Rhino7, the median surface was defined and exported as a Parasolid file to be imported into Patran for the creation of the FEM model. The mesh was created using both quadrangular elements (CQUAD4) and triangular elements (TRIA3). The thickness derived from the actual geometry is $2.5\,mm$. The same mechanical properties as for the previous case study are assumed.

The actual geometry has a total of six anchor points located as shown in the FEM model in Fig. 12. In the same

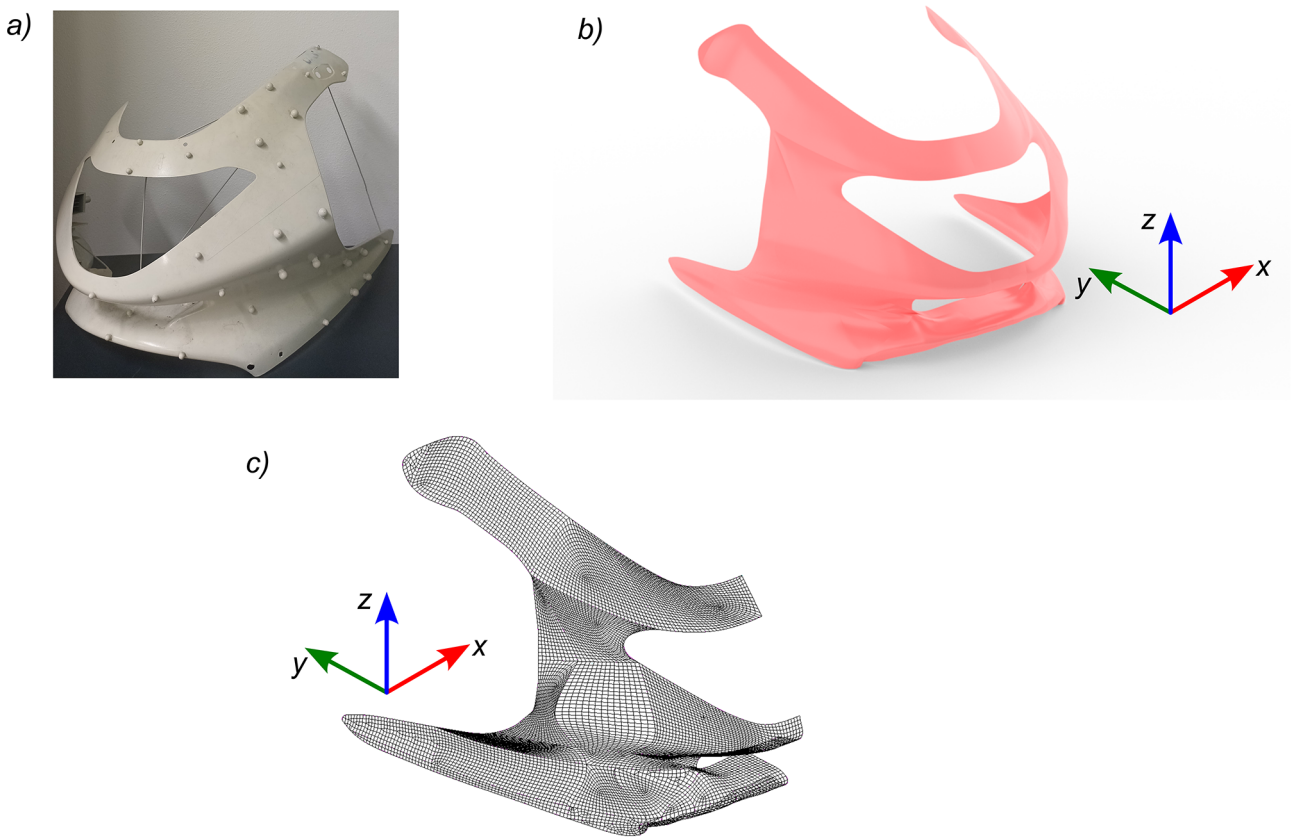

Fig. 11 Second case study actual part (**a**), CAD model (**b**), and FEM model (**c**)

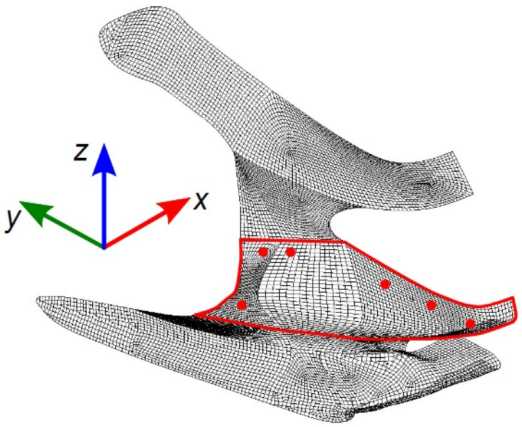

Fig. 12 Second case study original anchor points location, and admissible anchor point location subsequently used

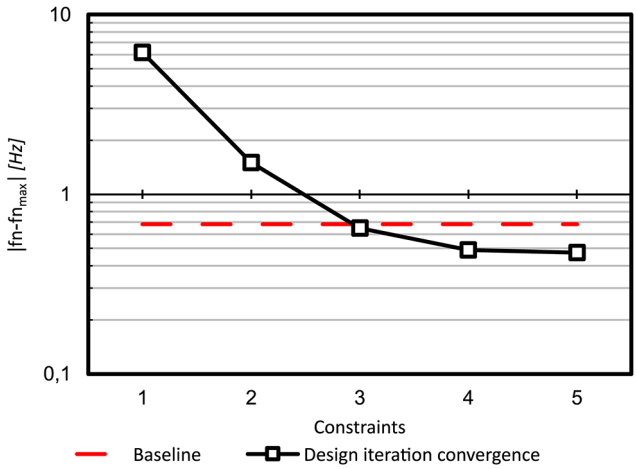

Fig. 13 Second case study results

figure, the admissible anchor point location is delimited. The baseline natural frequency is $6.89\,Hz$, and the maximum obtainable natural frequency is $7.57\,Hz$.

Using a starting point defined by the free state model analysis the result obtained can be seen in Fig. 13.

It can be noted that with three anchor points, a natural frequency greater than the baseline (6.89 Hz) can be reached by selecting the anchor point location according

to the proposed methodology. Figure 14 shows the location of these three anchor points and the corresponding modal analysis.

6 Discussion

The proposed methodology aims to provide designers with a formal approach to designing anchor points for deformable parts that need to achieve a stable configuration in their assembled state. The goal is to minimize the number of anchor points to simplify the assembly procedure and maximize the DfA index.

The procedure is inherently based on a worst-case scenario: it neglects the contact between parts, thereby underestimating the natural frequency and rigidity of the system. This fact implies considering only bilateral constraints and neglecting unilateral constraints. If full contact between the parts is considered, it limits the possible deformation of the part that is considered. As a consequence, the rigidity of the system is higher. Therefore, not considering the contact modelling in the FEM simulation coincide with considering a less rigid assembly, this condition is in safety favour. Furthermore, it is noteworthy to point out that the value of the methodology lies in its comparative analysis, so this limitation does not impede its implementation. However, further development of the methodology could investigate the effect of proper contact modelling in this design procedure. Contact modelling is crucial for all the methodologies dealing with the optimization of clamping and/or assembly sequences aiming to reduce and/or control geometrical deviation from nominal. In this case, since the actual value of the deviation is of interest, contact modelling becomes important.

The methodology, as presented in this work, is easy to implement for designers and requires no dedicated tools, except for FEM software, which is often available within standard CAD software packages [48].

In the validation example, it was shown that for a low number of constraints, the variability (standard deviation) of the natural frequency is high, up to almost 40% of the mean value. The dispersion considerably decreases for a higher number of constraints. Theoretically, for an infinite number of constraints, which represents glueing between parts along the entire possible connection area, the variability is zero. This indicates that for cases with a low number of connection points, there is room for further optimization of anchor locations to overcome the inherent sensitivity of the methodology to the initial anchor points.

Optimization routines require dedicated applications capable of performing optimization, making it less straightforward for designers. Nonetheless, it is worth exploring the possibility of creating an automatic tool in the future capable of finding the optimal location of a given number of constraints within the admissible domain. This can be achieved using a platform that enables CAD modelling, FEM simulations, and the ability to code an iterative routine to search for the optimum. The possibility of reaching a local optimum should be considered and automatically avoided.

Referring to the results of the validation case study, particularly Fig. 8, it's evident that the location of the anchor point determined by the methodology does not precisely match the optimal location. This discrepancy arises because adding a new constraint alters the modal deformation, implying that a specific optimum exists for each distinct number of constraints. The step-by-step procedure proposed in this work has the limitation of keeping the previously defined constraints fixed, thereby constraining the solution. However, it's worth noting that the point defined by the methodology is close to a local maximum and distant from local minimums, allowing for the implementation of

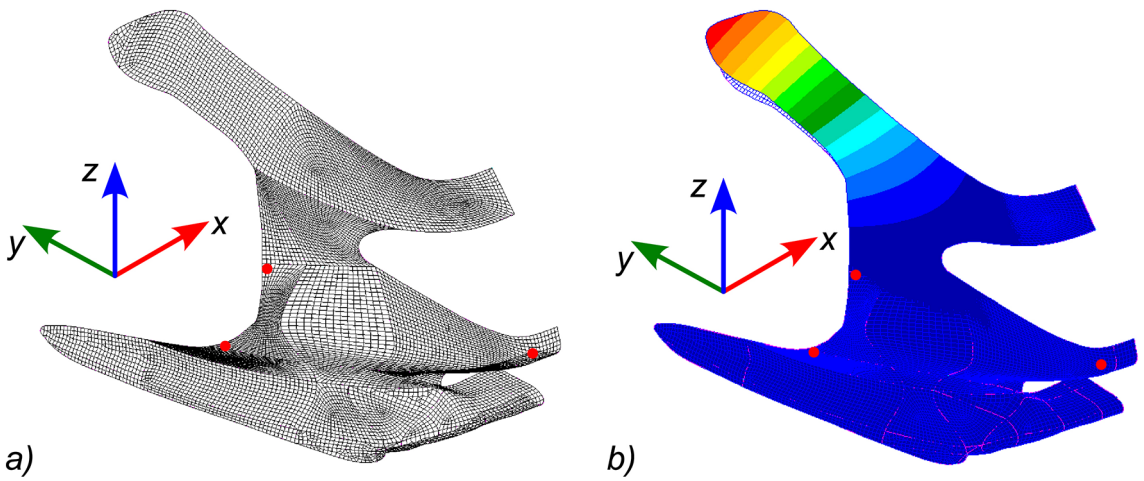

Fig. 14 Second case, **a**) location of three anchor points, and **b**) the correspondent modal analysis

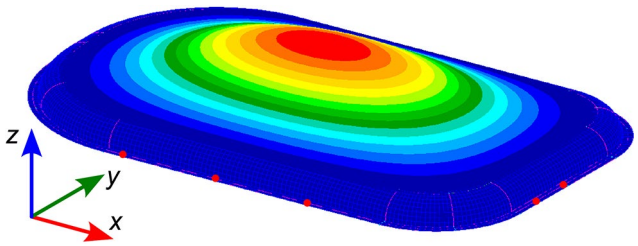

Fig. 15 First case study baseline simulation

an automated routine to search for the optimal point using differential analysis.

In the first case study, it's observed that the methodology fails to find a better solution than the existing design (achieving a greater or equal natural frequency with fewer anchor points). This limitation arises because the actual constraints enable the attainment of 98% of the maximum obtainable natural frequency. The modal analysis of the baseline case for the plastic cover is depicted in Fig. 15. Here, it can be observed that the part exhibits box-like behaviour, with vibrations limited to the central portion while the perimeter frame remains rigid. Adding further constraints and/or rearranging the existing ones can only marginally impact the natural frequency since the internal shell of the part remains unaffected by the modification.

This case might represent an overengineered part. It has been demonstrated that 95% of the baseline natural frequency can be achieved with seven constraints compared to the ten used in the baseline design. Another design issue might be represented by the fact that the part can be divided into two portions: the frame and the internal shell, where the frame is much stiffer than the other. Meanwhile, anchor points are only possible along the frame, meaning that the deformability of the internal shell is almost independent of the anchor point's location. A less rigid frame allows for better optimization of anchor point locations.

Looking at the second case study, it's evident that a drastic redesign is possible. The baseline design has a total of twelve anchor points, translating into six for the symmetric model used for the FEM analysis. Running the proposed methodology, a configuration with a total of 6 constraints (3 per side) can achieve a natural frequency higher than the baseline design. This means that such a configuration is much easier to assemble since only six shaft-hole connections/holes need to align compared to the baseline design which requires double the elements to align. The result is that the alignment time during assembly is lower. At the same time, assuming that only screws are used to lock in place the front fairing, the time to fasten the connection elements can be halved. This implies a significant impact on the DfA index.

The presented application might find several applications besides design. It can be used in production to determine the optimal fixturing of the workpiece during tooling. In this case, having simple fixturing allows for quicker production. Additionally, having the ability to evaluate the rigidity of the workpiece in its fixturing helps to avoid issues related to workpiece vibration relative to the tool, increasing production quality. Similarly, it can be used during inspection to evaluate the part placement and fixturing to decrease the uncertainty due to the deformability of the part. In this case, the aim is to simplify the placement and fixturing, allowing quicker and more reliable inspection.

7 Conclusions

This paper aims to propose a methodology to design the anchor points location for deformable parts that need to reach a stable configuration once assembled.

The proposed methodology is relevant for the design phase when the designer is tasked with creating a nominal geometry fulfilling functional requirements. Designers using the proposed methodology can define the minimum number of anchor points fulfilling the desired final rigidity of the assembly. By doing so, the assembly process becomes easier for fewer features to be aligned and/or fewer connections to be used. As a consequence, the assembly time can be minimized therefore maximising the DfA index. Besides this application, in the Discussion section, further possible applications relevant to manufacturing and quality control departments are provided.

The methodology was validated through a simple case study where different settings for the methodology were tested. It was shown that the methodology exhibits an asymptotic trend towards the maximum obtainable natural frequency. Furthermore, different settings converge to the same, or very similar, final solutions. The variability among different settings opens the possibility to explore possible refinements to the methodology, exploring optimization routines to find, for each number of anchor points, the global maximum natural frequency, and therefore rigidity.

Two increasingly complex case studies were also presented and studied. In particular, referencing the motorcycle front fairing, applying the methodology made it possible to achieve the same rigidity with fewer than half the anchor points of the original design, proving its effectiveness.

Funding The authors have no relevant financial or non-financial interests to disclose.
Open access funding provided by Università degli Studi di Padova within the CRUI-CARE Agreement.

References

1. Ostermann, M., Grenz, J., Triebus, M., Cerdas, F., Marten, T., Tröster, T., Herrmann, C.: Integrating prospective scenarios in Life Cycle Engineering: Case Study of Lightweight structures. Energies. **16**, 3371 (2023). https://doi.org/10.3390/en16083371
2. Koffler, C., Rohde-Brandenburger, K.: On the calculation of fuel savings through lightweight design in automotive life cycle assessments. Int. J. Life Cycle Assess. **15**, 128–135 (2010). https://doi.org/10.1007/s11367-009-0127-z
3. Altenbach, H., Eremeyev, V.: Thin-Walled Structural Elements: Classification, Classical and Advanced Theories, New Applications, in: : pp. 1–62. (2017). https://doi.org/10.1007/978-3-319-42277-0_1
4. Qi, C., Jiang, F., Yang, S.: Advanced honeycomb designs for improving mechanical properties: A review, Compos. Part. B Eng. **227**, 109393 (2021). https://doi.org/10.1016/j.compositesb.2021.109393
5. Maltauro, M., Passarotto, G., Concheri, G., Meneghello, R.: Bridging the gap between design and manufacturing specifications for non-rigid parts using the influence coefficient method. Int. J. Adv. Manuf. Technol. **127**, 579–597 (2023). https://doi.org/10.1007/s00170-023-11480-4
6. Sellem, E., Rivière, A.: Tolerance Analysis of Deformable Assemblies, in: Vol. 2 24th Des. Autom. Conf., American Society of Mechanical Engineers, (1998). https://doi.org/10.1115/DETC98/DAC-5571
7. Charles Liu, S., Jack, S., Hu: An offset finite element model and its applications in predicting sheet metal assembly variation. Int. J. Mach. Tools Manuf. **35**, 1545–1557 (1995). https://doi.org/10.1016/0890-6955(94)00103-Q
8. Liu, S.C., Hu, S.J., Woo, T.C.: Tolerance Analysis for Sheet Metal Assemblies. J. Mech. Des. **118**, 62–67 (1996). https://doi.org/10.1115/1.2826857
9. Liu, S.C., Hu, S.J.: Variation Simulation for Deformable Sheet Metal Assemblies using Finite element methods. J. Manuf. Sci. Eng. **119**, 368–374 (1997). https://doi.org/10.1115/1.2831115
10. Atik, H., Chahbouni, M., Amegouz, D., Boutahari, S.: Optimization tolerancing of surface in flexible parts and assembly: Influence coefficient method with shape defects. Int. J. Eng. Technol. **7**, 90 (2018). https://doi.org/10.14419/ijet.v7i1.8470
11. Atik, H., Chahbouni, M., Amagouz, D., Boutahari, S.: An analysis of springback of compliant assemblies by contact modeling and welding distortion. Int. J. Eng. Technol. **7**, 85 (2018). https://doi.org/10.14419/ijet.v7i1.8330
12. Polini, W., Corrado, A.: Methods of influence coefficients to evaluate stress and deviation distribution of flexible assemblies—a review. Int. J. Adv. Manuf. Technol. **107**, 2901–2915 (2020). https://doi.org/10.1007/s00170-020-05210-3
13. Chang, M., Gossard, D.C.: Modeling the assembly of compliant, non-ideal parts. Comput. Des. **29**, 701–708 (1997). https://doi.org/10.1016/S0010-4485(97)00017-1
14. Cai, W., Hu, S.J., Yuan, J.X.: A Variational Method of Robust Fixture Configuration Design for 3-D Workpieces. J. Manuf. Sci. Eng. **119**, 593–602 (1997). https://doi.org/10.1115/1.2831192
15. Yao, S., Luan, Y., Ceccarelli, M., Carbone, G.: Optimization method of the Clamping Force for large cabin parts. Appl. Sci. **13**, 12575 (2023). https://doi.org/10.3390/app132312575
16. Maropoulos, P.G., Vichare, P., Martin, O., Muelaner, J., Summers, M.D., Kayani, A.: Early design verification of complex assembly variability using a hybrid – model based and physical testing – methodology. CIRP Ann. **60**, 207–210 (2011). https://doi.org/10.1016/j.cirp.2011.03.097
17. Raghu, A., Melkote, S.N.: Analysis of the effects of fixture clamping sequence on part location errors. Int. J. Mach. Tools Manuf. **44**, 373–382 (2004). https://doi.org/10.1016/j.ijmachtools.2003.10.015
18. Li, B., Melkote, S.N.: Improved workpiece location accuracy through fixture layout optimization. Int. J. Mach. Tools Manuf. **39**, 871–883 (1999). https://doi.org/10.1016/S0890-6955(98)00072-8
19. Matuszyk, T.I., Cardew-Hall, M., Rolfe, B.F.: The effect of clamping sequence on dimensional variability in sheet metal assembly. Virtual Phys. Prototyp. **2**, 161–171 (2007). https://doi.org/10.1080/17452750701677467
20. Sadeghi Tabar, R., Lorin, S., Cromvik, C., Lindkvist, L., Wärmefjord, K., Söderberg, R.: Efficient spot welding sequence Simulation in Compliant Variation Simulation. J. Manuf. Sci. Eng. **143** (2021). https://doi.org/10.1115/1.4049654
21. Choi, W., Chung, H.: Variation Simulation of compliant metal plate assemblies considering welding distortion. J. Manuf. Sci. Eng. **137** (2015). https://doi.org/10.1115/1.4029755
22. Zheng, H., Litwa, F., Bohn, M., Paetzold, K.: Tolerance optimization for sheet metal parts based on joining simulation. Procedia CIRP. **100**, 583–588 (2021). https://doi.org/10.1016/j.procir.2021.05.127
23. Moos, S., Vezzetti, E.: Compliant assembly tolerance analysis: Guidelines to formalize the resistance spot welding plasticity effects. Int. J. Adv. Manuf. Technol. **61**, 503–518 (2012). https://doi.org/10.1007/s00170-011-3729-0
24. Camelio, J., Hu, S.J., Ceglarek, D.: Modeling variation propagation of Multi-station Assembly systems with compliant parts. J. Mech. Des. **125**, 673–681 (2003). https://doi.org/10.1115/1.1631574
25. Tabar, R.S., Lindkvist, L., Wärmefjord, K., Söderberg, R.: Efficient joining sequence variation analysis of stochastic batch assemblies. J. Comput. Inf. Sci. Eng. **22** (2022). https://doi.org/10.1115/1.4054000
26. Lu, C., Zhao, H.-W.: Fixture layout optimization for deformable sheet metal workpiece. Int. J. Adv. Manuf. Technol. **78**, 85–98 (2015). https://doi.org/10.1007/s00170-014-6647-0
27. Sadeghi Tabar, R., Zheng, H., Litwa, F., Paetzold-Byhain, K., Lindkvist, L., Wärmefjord, K., Söderberg, R.: Digital Twin-based clamping sequence analysis and optimization for Improved Geometric Quality. Appl. Sci. **14**, 510 (2024). https://doi.org/10.3390/app14020510
28. Radvar-Esfahlan, H., Tahan, S.-A.: Nonrigid geometric metrology using generalized numerical inspection fixtures. Precis Eng. **36**, 1–9 (2012). https://doi.org/10.1016/j.precisioneng.2011.07.002
29. Sabri, V., Tahan, S.A., Pham, X.T., Moreau, D., Galibois, S.: Fixtureless profile inspection of non-rigid parts using the numerical inspection fixture with improved definition of displacement boundary conditions. Int. J. Adv. Manuf. Technol. **82**, 1343–1352 (2016). https://doi.org/10.1007/s00170-015-7425-3
30. Sabri, V., Sattarpanah, S., Tahan, S.A., Cuillière, J.C., François, V., Pham, X.T.: A robust and automated FE-based method for fixtureless dimensional metrology of non-rigid parts using an improved numerical inspection fixture. Int. J. Adv. Manuf. Technol. **92**, 2411–2423 (2017). https://doi.org/10.1007/s00170-017-0216-2

31. Lindau, B., Wärmefjord, K., Lindkvist, L., Söderberg, R.: Virtual fixturing: Inspection of a Non-rigid Detail resting on 3-Points to Estimate Free State and Over-constrained Shapes. In: Vol. 2B Adv. Manuf. American Society of Mechanical Engineers (2020). https://doi.org/10.1115/IMECE2020-24515
32. Morse, E., Grohol, C.: Practical conformance evaluation in the measurement of flexible parts. CIRP Ann. **68**, 507–510 (2019). https://doi.org/10.1016/j.cirp.2019.04.076
33. Maltauro, M., Meneghello, R., Concheri, G.: Conformity Rate Estimation for Shaft-Hole Pattern Fit Not Compliant with the Boundary Condition Design Criterion, in: S. Gerbino, A. Lanzotti, M. Martorelli, R. Mirálbes Buil, C. Rizzi, L. Roucoules (Eds.), Adv. Mech. Des. Eng. Manuf. IV - Proc. Int. Jt. Conf. Mech. Des. Eng. Adv. Manuf. JCM 2022, June 1–3, 2022, Ischia, Italy, Springer International Publishing, Cham, : pp. 1256–1267. (2023). https://doi.org/10.1007/978-3-031-15928-2_110
34. Boothroyd, G.: Design for manufacture and assembly: The Boothroyd-Dewhurst experience. In: Des. X, pp. 19–40. Springer Netherlands, Dordrecht (1996). https://doi.org/10.1007/978-94-011-3985-4_2
35. Boothroyd, G., Knight, W.: Design for assembly. IEEE Spectr. **30**, 53–55 (1993). https://doi.org/10.1109/6.275164
36. Boothroyd, G.: Design for assembly—the key to design for manufacture. Int. J. Adv. Manuf. Technol. **2**, 3–11 (1987). https://doi.org/10.1007/BF02601481
37. Boothroyd, G., Alting, L.: Design for Assembly and Disassembly. CIRP Ann. **41**, 625–636 (1992). https://doi.org/10.1016/S0007-8506(07)63249-1
38. Formentini, G., Boix Rodríguez, N., Favi, C.: Design for manufacturing and assembly methods in the product development process of mechanical products: A systematic literature review. Int. J. Adv. Manuf. Technol. **120**, 4307–4334 (2022). https://doi.org/10.1007/s00170-022-08837-6
39. Suresh, P., Ramabalan, S., Natarajan, U.: Integration of DFE and DFMA for the sustainable development of an automotive component. Int. J. Sustain. Eng. **9**, 107–118 (2016). https://doi.org/10.1080/19397038.2015.1096313
40. Bouissiere, F., Cuiller, C., -E Dereux, P., Malchair, C., Favi, C., Formentini, G.: Conceptual Design for Assembly in Aerospace Industry: A method to assess Manufacturing and Assembly aspects of product architectures. Proc. Des. Soc. Int. Conf. Eng. Des. 1. **2961–2970** (2019). https://doi.org/10.1017/dsi.2019.303
41. Zhai, Y., Sun, Y., Li, Y., Tang, S.: Design for Assembly (DFA) evaluation method for Prefabricated buildings. Buildings. **13**, 2692 (2023). https://doi.org/10.3390/buildings13112692
42. Gao, S., Jin, R., Lu, W.: Design for manufacture and assembly in construction: A review. Build. Res. Inf. **48**, 538–550 (2020). https://doi.org/10.1080/09613218.2019.1660608
43. Sąsiadek, M., Niedziela, M., Woźniak, W., Jachowicz, T., Mikušová, N.: A New Effective Algorithm for Mechanical Assembly sequence planning. Adv. Sci. Technol. Res. J. **17**, 56–67 (2023). https://doi.org/10.12913/22998624/171271
44. You, W.-H., Jung, Y.-H., Koo, J.-S.: Vibration reduction of Pipe line in air-conditioner for Railway Vehicle. Trans. Korean Soc. Noise Vib. Eng. **22**, 925–931 (2012). https://doi.org/10.5050/KSNVE.2012.22.10.925
45. Wang, M., Chen, X., Li, X.: An Ultra-low frequency two DOFs' vibration isolator using positive and negative stiffness in parallel. Math. Probl. Eng. **2016**, 1–15 (2016). https://doi.org/10.1155/2016/3728397
46. Zanardo, G., Hao, H., Xia, Y., Deeks, A.J.: Stiffness Assessment through Modal Analysis of an RC Slab Bridge before and after strengthening. J. Bridg Eng. **11**, 590–601 (2006). https://doi.org/10.1061/(ASCE)1084-0702(2006)11:5(590)
47. Martin, R.R., Dutta, D.: Tools for Asymmetry Rectification in Shape Design, J. Syst. Eng. 6 98–112. (1996). https://citeseerx.ist.psu.edu/document?repid=rep1&type=pdf&doi=39339c42526ff9342e67bc480c4b9a8995881a38
48. Shaisundaram, V.S., Karikalan, L., Ramasubramanian, S., Baskar, S., Balaji, R.: Design and Analysis of a Panel Using FEA, in: : pp. 31–37. (2022). https://doi.org/10.1007/978-981-19-0244-4_5